

# Zooming in on a sleeping giant: milliarcsecond HSA imaging of the black hole binary V404 Cyg in quiescence

J.C.A. Miller-Jones,<sup>1,2\*</sup> E. Gallo,<sup>3,4</sup> M.P. Rupen,<sup>5</sup> A.J. Mioduszewski,<sup>5</sup>  
W. Briskin,<sup>1</sup> R.P. Fender,<sup>6,7</sup> P.G. Jonker,<sup>8,9,10</sup> and T.J. Maccarone,<sup>6</sup>

<sup>1</sup>*NRAO Headquarters, 520 Edgemont Road, Charlottesville, VA, 22903, USA*

<sup>2</sup>*Jansky Fellow, National Radio Astronomy Observatory*

<sup>3</sup>*Physics Department, Broida Hall, University of California, Santa Barbara, CA, 93106, USA*

<sup>4</sup>*Chandra Fellow*

<sup>5</sup>*NRAO, Array Operations Center, 1003 Lopezville Road, Socorro, NM 87801, U.S.A.*

<sup>6</sup>*School of Physics and Astronomy, University of Southampton, Highfield, Southampton, SO17 1BJ*

<sup>7</sup>*Astronomical Institute ‘Anton Pannekoek’, University of Amsterdam, Kruislaan 403, 1098 SJ, Amsterdam, The Netherlands*

<sup>8</sup>*SRON, Netherlands Institute for Space Research, 3584 CA Utrecht, The Netherlands*

<sup>9</sup>*Harvard-Smithsonian Center for Astrophysics, Cambridge, MA 02138, USA*

<sup>10</sup>*Astronomical Institute, Utrecht University, 3508 TA, Utrecht, The Netherlands*

Accepted xxxxxxx. Received xxxxxxx; in original form xxxxxxx

## ABSTRACT

Observations of the black hole X-ray binary V404 Cyg with the very long baseline interferometer HSA (the High Sensitivity Array) have detected the source at a frequency of 8.4 GHz, providing a source position accurate to 0.3 mas relative to the calibrator source. The observations put an upper limit of 1.3 mas on the source size (5.2 AU at 4 kpc) and a lower limit of  $7 \times 10^6$  K on its brightness temperature during the normal quiescent state, implying that the radio emission must be non-thermal, most probably synchrotron radiation, possibly from a jet. The radio lightcurves show a short flare, with a rise time of  $\sim 30$  min, confirming that the source remains active in the quiescent state.

**Key words:** X-rays: binaries – radio continuum: stars – stars: individual (V404 Cyg) – ISM: jets and outflows – astrometry

## 1 INTRODUCTION

Accreting black hole X-ray binary systems spend the majority of their time in the so-called “quiescent” state, a low-luminosity state (below a few  $\times 10^{-6}$  of the Eddington luminosity) whose X-ray emission is characterised by a hard ( $1.5 < \Gamma < 2.1$ ) power-law spectrum (McClintock & Remillard 2006). Despite such highly sub-Eddington systems being so numerous, their intrinsic faintness poses serious observational challenges to any attempt to understand the nature of the accretion flow in these systems.

Accreting black holes have been studied in much more depth in the “hard” state, a regime with a similarly hard spectrum but occurring at higher X-ray luminosities (up to a few per cent of the Eddington luminosity). In this state, they show flat radio spectra, (e.g Fender 2001) interpreted as synchrotron emission arising from partially self-absorbed, conical jets (Blandford & Konigl 1979; Hjellming & Johnston 1988). Such jet-like structures have been directly imaged

in two systems, GRS 1915+105 (Dhawan et al. 2000) and Cygnus X-1 (Stirling et al. 2001), at X-ray luminosities of 5 and 0.3 per cent of the Eddington luminosity respectively. With only two relatively luminous examples of self-absorbed jets, it has not been possible to study the dependence of the jet size and geometry with system parameters such as orbital period, nature of the mass donor, accretion rate, and black hole mass.

On moving from the hard to the quiescent state, the radio properties of X-ray binaries become progressively less constrained, owing to the limitations of current instrumentation. In particular, the questions of whether radio-emitting outflows persist into quiescence, and if so, what form they take, remain to be answered. Quiescence is currently defined (McClintock & Remillard 2006) only by the luminosity criterion  $L_x < 10^{33.5} \text{ erg s}^{-1}$  (i.e.  $L_x/L_{\text{Edd}} < 2.3 \times 10^{-6} (M_{\text{BH}}/10M_{\odot})$ , where  $L_{\text{Edd}}$  is the Eddington luminosity and  $M_{\text{BH}}$  is the black hole mass), although there are indications that the X-ray spectrum in quiescence softens from the canonical power-law index  $\Gamma \sim 1.5$  of the hard state to a value closer to 2 (Gallo et al. 2006; Corbel et al.

\* email: jmiller@nrao.edu

2006; Bradley et al. 2007). However, at such low luminosities, instrumental sensitivity begins to hamper efforts to characterise the behaviour of quiescent systems, and the detailed spectral properties of the quiescent state remain to be determined. Extrapolation of the observed hard state behaviour suggests that it is a reasonable assumption that jets should also exist in the quiescent state. This hypothesis is supported by the detection of A0620-00 in the quiescent state in both the radio and X-ray bands (Gallo et al. 2006), which demonstrated that the radio/X-ray correlation seen in the hard state (Gallo et al. 2003) remains unbroken down to  $10^{-8.5} L_{\text{Edd}}$ . Further support is provided by the observed flat radio spectrum in V404 Cyg (Gallo et al. 2005). However, the evidence is circumstantial, and direct empirical proof for the existence of such quiescent jets is still lacking.

### 1.1 V404 Cyg

V404 Cyg (GS 2023+338) is the most luminous of the quiescent black hole X-ray binaries, with a mean X-ray luminosity of  $\sim 10^{33}(d/4\text{kpc})^2 \text{ erg s}^{-1}$  (Garcia et al. 2001; Kong et al. 2002; Hynes et al. 2004; Bradley et al. 2007). Its high, accurately-determined mass function,  $6.08 \pm 0.06 M_{\odot}$  (the most statistically significant measurement of a mass function above  $3M_{\odot}$ ; Casares & Charles 1994), implies that the compact object must be a black hole. The best-fitting system parameters indicate that the mass donor is a K0 IV star (Casares et al. 1993) in a 6.5-d orbit with a black hole of mass  $12 \pm 2 M_{\odot}$  (Shahbaz et al. 1994), although contamination of the infrared spectrum by light from the accretion disc could reduce this to  $10 M_{\odot}$ , with a firm lower limit of  $7.4 M_{\odot}$  (Shahbaz et al. 1996). Han & Hjellming (1992) measured a kinematic HI distance of  $d \geq 3.2 \text{ kpc}$ . Assuming Eddington-limited X-ray emission during the 1989 outburst gives a maximum distance of  $\leq 3.7 \text{ kpc}$ , whereas the optical magnitude and reddening information suggests  $d = 4.0_{-1.2}^{+2.0} \text{ kpc}$  (Jonker & Nelemans 2004). We will adopt the latter value for the rest of this work.

The radio spectrum of V404 Cyg was measured to be flat, with a spectral index of  $\alpha = 0.09 \pm 0.19$  (Gallo, Fender & Hynes 2005), defining  $S_{\nu} \propto \nu^{\alpha}$ . Its flux density is  $\sim 0.3 \text{ mJy}$  at radio wavelengths (Gallo, Fender & Pooley 2003), although it is known to vary up to levels of  $1.5 \text{ mJy}$  (Hjellming et al. 2000). The radio emission is believed to be of synchrotron origin (Gallo et al. 2005), and the quiescent radio and X-ray luminosities are consistent with an extrapolation of the non-linear radio/X-ray correlation found for hard state X-ray binaries (Gallo et al. 2003), suggestive of jet emission. However, the collimated nature of the outflow remains to be proven.

Muno & Mauerhan (2006) detected 4.5- and 8- $\mu\text{m}$  infrared emission from V404 Cyg in excess of that expected from the Rayleigh-Jeans tail of the companion star, which they attributed to emission from the accretion disc. However, Gallo et al. (2007) demonstrated that the broadband radio through X-ray spectral energy distribution (SED) could be well fitted with a maximally jet-dominated model, suggesting that the excess infrared emission was consistent with being synchrotron emission from a partially self-absorbed jet.

As the most luminous quiescent black hole X-ray binary, and with so much circumstantial evidence for jets, V404 Cyg

is the ideal candidate in which to try to demonstrate empirically the existence of jets in a quiescent accreting black hole system. Since the source is so faint ( $\sim 0.3 \text{ mJy}$ ; other quiescent systems are fainter still), we proposed for Very Long Baseline Interferometry (VLBI) observations with the High Sensitivity Array (HSA) in an attempt to resolve the jets, and as a pilot to check the feasibility of a future parallax measurement to determine the source distance.

## 2 OBSERVATIONS AND DATA REDUCTION

V404 Cyg was observed for 4.25 h with the HSA on 2007 December 2, from 18:00:00 until 22:15:00 UT, under program code BG 168. We used nine antennas of the Very Long Baseline Array (VLBA; the tenth antenna, St. Croix, was down for maintenance) plus the Green Bank Telescope (GBT), Effelsberg and the phased Very Large Array (VLA). Eleven of the 24 available VLA stations were retrofitted EVLA antennas. We observed at 8.4 GHz, in dual-circular polarization, with a bandwidth of 32 MHz per polarization. Samples were quantized to 2-bits, giving a total bit rate of  $256 \text{ Mb s}^{-1}$ . We used J 2025+3343, a 2-Jy source located only 16.6 arcmin from the target, as both the fringe finder and phase reference source. We observed in 3-min cycles, spending 2 min on the target and 1 min on the calibrator in each cycle. Every 24 min, we also made observations of a check source, J 2023+3153, the next nearest bright calibrator ( $1.9^{\circ}$  from the phase reference source), followed by a rephasing of the VLA.

Data were reduced according to standard procedures within the National Radio Astronomy Observatory's Astronomical Image Processing System (AIPS) software (Greisen 2003). During the self-calibration of the phase reference source, the initial model of the calibrator was created using only the VLBA antennas, since the a priori calibration (using system temperatures) for the VLBA antennas is better than that for the larger dishes. Amplitude self-calibration was then used to correct the gains of the large dishes according to the VLBA-only model. Since the sensitivities on the typically long baselines connecting the large dishes dominated the self-calibration solutions, their absolute flux scale could not be sufficiently well determined using standard calibration. The visibilities on baselines from the Los Alamos (LA) station to the VLA were compared to those at similar  $(u, v)$  co-ordinates between the LA and Pie Town (PT) stations, and a global scaling factor of 0.89 was applied to correct the VLA gains and bring the two sets of visibilities into agreement. A similar procedure was applied to baselines from the North Liberty (NL) station to both the Hancock (HN) antenna and the GBT, although it was found that no scaling was necessary for the GBT gains. Finally, the calibration derived on the phase reference source was transferred to the target. Owing to the low flux density of the target, no self-calibration was performed.

The extreme scattering towards the phase reference source (Fey et al. 1989) meant that the achievable resolution was set by the longest unscattered baseline to the calibrator, rather than the expected instrumental resolution. For this reason, the data from Effelsberg had to be rejected. Visibilities were scattered to zero amplitudes on baselines longer than  $150 \text{ M}\lambda$  (Fig. 1), whereas baselines to Effelsberg were

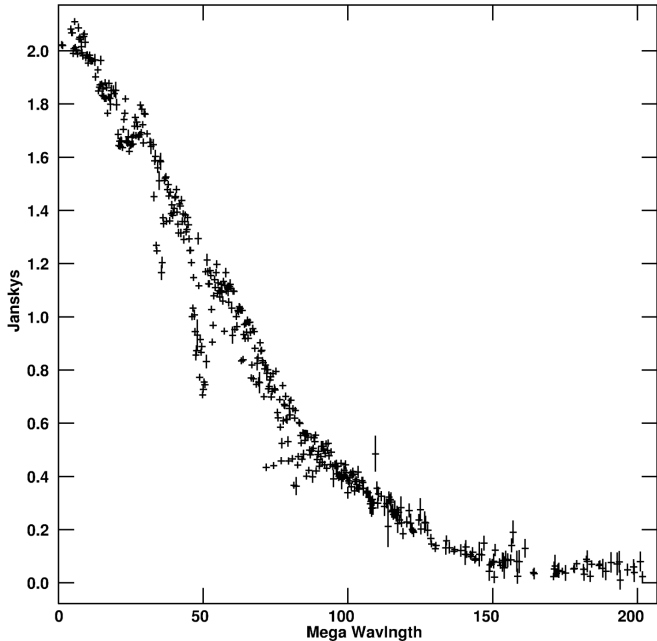


**Figure 1.** Amplitude of the real part of the visibility plotted against radial distance from the centre of the  $uv$ -plane, for the phase reference source J2025+3343. The shape of the plot is consistent with anisotropic interstellar scattering (as parameterised by, e.g., Desai & Fey 2001) giving rise to an elliptical scattering disc of size  $2.2 \times 1.4$  mas in PA  $2^\circ$  (see Section 5), with the power-law index of the electron density fluctuations in the interstellar medium being close to 4, as found for J2025+3343 by Fey et al. (1989).

between 120 and 290 M $\lambda$ . Those in the range 120–150 M $\lambda$  were taken at the lowest elevations, and it was not deemed possible to achieve accurate gain calibration for any of the data from this station.

The VLA data were independently reduced and imaged, using standard procedures within AIPS. Weather conditions at the VLA were excellent throughout the observations. Amplitude calibration was performed using observations of 3C 48, adopting the flux density scale set by the coefficients derived at the VLA in 1999.2, as implemented in the 31DEC08 version of AIPS. While no proper polarization calibration could be performed, the low polarization leakage of the VLA (of order a few per cent) meant that we could obtain approximate constraints on the linear ( $P$ ) and circular ( $V$ ) polarization of the source by imaging the two internal IF pairs separately in all four Stokes parameters  $I$ ,  $Q$ ,  $U$  and  $V$ , and forming  $P = (Q^2 + U^2)^{1/2}$ .

### 3 RESULTS

V404 Cyg was detected by the HSA at a  $12\sigma$  level with a mean flux density of  $0.32 \pm 0.03$  mJy  $\text{bm}^{-1}$  (here and in all the following sections, unless specified, we quote  $1\sigma$  error bars). The source was unresolved down to a beamsize of  $5.0 \times 1.4$  mas $^2$  in PA  $2^\circ 0$  (Fig. 2). The elongation is caused by the high sensitivities of the GBT and phased VLA, with baselines to (and particularly between) those antennas dominating the naturally-weighted sampling function.

We independently reduced the VLA data, to measure

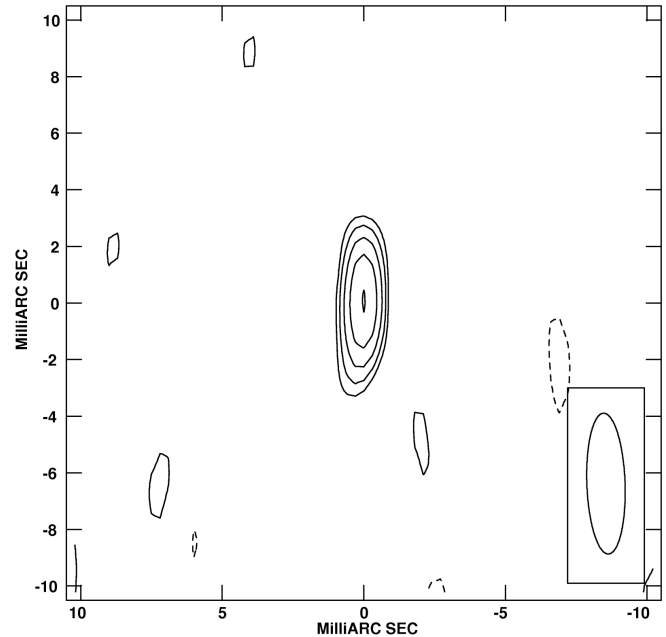


**Figure 2.** Image of V404 Cyg. The beamsize ( $5.0 \times 1.4$  mas $^2$  in PA  $2^\circ 0$ ) is shown in the lower right. Contours are at levels of  $\pm(\sqrt{2})^n$  times the rms noise in the image ( $0.027$  mJy  $\text{bm}^{-1}$ ), where  $n = 3, 4, 5, \dots$ , with the lowest contour being at  $0.078$  mJy  $\text{bm}^{-1}$ , and the peak flux density in the image being  $0.322$  mJy  $\text{bm}^{-1}$ . The source is unresolved.

the total flux density of the source and ascertain whether any emission was being resolved out by the HSA. The flux density measured by the VLA, averaged over the length of the observation, was  $0.47 \pm 0.03$  mJy, showing that the HSA is detecting most of the flux density, and constraining the majority of the emission to come from a region smaller than 5 mas (Section 4 discusses the size constraint in more detail).

#### 3.1 Variability

To search for shorter-timescale variability, the VLA data were split into short (30-min) time segments and imaged. The source was fit in the image plane with a point source model during each 30-min interval, and the resulting lightcurve is shown in Fig. 3.

The measured HSA flux density is consistent with recovering  $\sim 70$  per cent of the total flux density measured with the VLA at all times. When imaging the data from the flare at the end of the observations, editing out the data from the phased VLA resulted in recovering a much higher fraction of the total source flux ( $1.00 \pm 0.14$  mJy out of  $1.14 \pm 0.07$  mJy), suggesting possible amplitude calibration or phasing problems with the VLA. However, a similar analysis performed on the non-flare data showed no significant discrepancy between the results with and without including the phased VLA. Thus any problems with the phased VLA were confined to the time of the flaring observations.

##### 3.1.1 Flaring emission

The source flux density as measured by the VLA rose by a factor of 3 during the flare at the end of the ob-

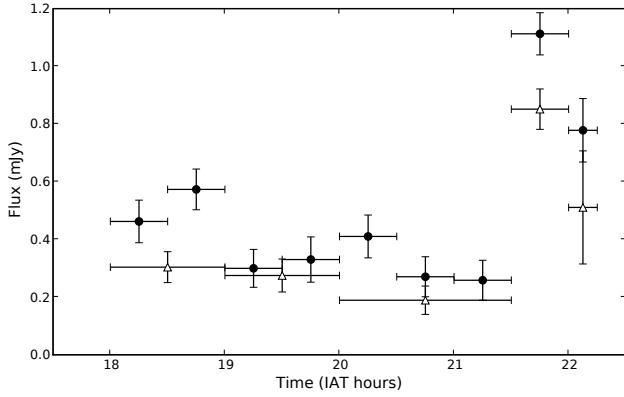


**Figure 3.** VLA (filled circles) and HSA (open triangles) lightcurves during the HSA observations of V404 Cyg. Note the flare at the end of the observations.

serving run, and there is also the suggestion of a smaller flare earlier in the observation, at 18:45. The rise time of the main flare was  $< 30$  min, and it showed no detectable circular or linear polarization (to a  $5\sigma$  limit of 32 per cent), ruling out coherent stellar bursts from the donor as the origin of the emission. However, incoherent gyrosynchrotron stellar flares with timescales of tens of minutes and much lower degrees of circular polarization are common in RS CVn and Algol-type systems (Güdel 2002), and the peak radio luminosities of such flares can reach levels of  $10^{17}$ – $10^{18}$   $\text{erg s}^{-1} \text{Hz}^{-1}$  (e.g. Mutel et al. 1987; Benz & Güdel 1994; García-Sánchez et al. 2003). One such system, UX Ari, with a K0 subgiant in a 6.44-d orbital period with a G5 main sequence star (Strassmeier et al. 1993), makes for a good comparison to V404 Cyg in terms of the rotation rate and stellar type of the flaring subgiant star. The maximum flare strength seen in this system in 3 years of radio monitoring was 0.82 Jy at 8.3 GHz (Richards et al. 2003), implying a peak luminosity of  $2.5 \times 10^{18}$   $\text{erg s}^{-1} \text{Hz}^{-1}$ , among the highest observed to date in such systems. The peak luminosity of the flare seen in V404 Cyg was an order of magnitude higher still, making it unlikely (if not impossible) that the observed flare in our data originates from the donor star.

Splitting the HSA observations into 1-h chunks for imaging (Fig. 3), we found that the flare was also seen in the high-resolution data. Imaging only the data from during the flare also showed that the source was unresolved, being smaller than the beamsize of  $4.7 \times 1.1 \text{ mas}^2$  in PA  $-5^\circ.9$ .

### 3.1.2 Non-flaring emission

Taking only the data prior to the flare (18:00–21:30 UT), the HSA measured a mean quiescent flux density of  $0.24 \pm 0.03 \text{ mJy beam}^{-1}$ , and the source was unresolved with a beamsize of  $5.2 \times 1.4 \text{ mas}^2$  in PA  $5^\circ.5$ . The VLA alone measured  $0.35 \pm 0.03 \text{ mJy beam}^{-1}$ . There was no evidence for any source polarization with the VLA, down to a  $5\sigma$  limit of 40 per cent for both linear and circular polarization.

## 3.2 Source position

The shift in source position between quiescent and flaring states was  $0.13 \pm 0.31 \text{ mas}$  ( $1\sigma$  uncertainty), consistent with zero. Using all the available data, the measured VLBI position, relative to the phase reference source J 2025+3343 (whose position was taken to be<sup>1</sup> (J 2000)  $20^{\text{h}}25^{\text{m}}10^{\text{s}}.8421050(224) 33^\circ 43'00''.21443(42)$ ) was

$$\text{RA} = 20^{\text{h}}24^{\text{m}}03^{\text{s}}.821269 \pm 0.000004$$

$$\text{Dec.} = +33^\circ 52'01''.8988 \pm 0.0002 \quad (\text{J 2000}),$$

where the quoted error bars are the purely statistical errors from fitting in the image plane. Imaging of the check source, J 2023+3153, phase referenced to J 2025+3343, showed that the shift in its position, relative to the catalogued position, was 0.34 mas in RA and 0.09 mas in Dec., compared to uncertainties of 0.24 and 0.41 mas respectively in the catalogued position of J 2023+3153. Since the check source was seven times further away from the phase reference calibrator than the target source, we are therefore confident that the systematic errors in the source position (e.g. due to atmospheric phase gradients) are small and the positional uncertainty is dominated by the signal-to-noise ratio on the target.

The unresolved nature of the source makes this system a good candidate for a future parallactic distance determination, free from the extra positional uncertainties introduced by source structure. The current measurement of the position would be used as an initial starting point. A distance of  $4.0_{-1.2}^{+2.0}$  kpc (Jonker & Nelemans 2004) would imply a parallax of  $\pi = 0.25_{-0.08}^{+0.13}$  mas, which is certainly feasible with current instrumentation.

## 4 JET SIZE CONSTRAINTS

### 4.1 Image and visibility-based limits

In order to put limits on the size of any extension, we fitted the source with an elliptical Gaussian in both the image plane (with the AIPS task JMFIT) and the  $uv$ -plane (using the AIPS task UVFIT and the Caltech VLBI package Difmap). Using the whole data set with all available stations, the ( $1\sigma$ ) upper limit on the FWHM of the major axis was found to be  $\sim 1.3 \text{ mas}$ . We note that a sufficiently low-level extension would not show up in the fitting results, so this is not a rigorous upper limit to the source size.

### 4.2 Brightness temperature limits

Radio surface brightness may be parameterized in terms of the temperature a blackbody would need to have in order to produce a source of the observed size and flux density, at the observed frequency, in the Rayleigh-Jeans limit. This is the brightness temperature, given by

$$T_{\text{b}} = \frac{c^2 S_{\nu}}{2\nu^2 k_{\text{B}} \Omega}, \quad (1)$$

where  $c$  is the speed of light,  $S_{\nu}$  the source flux density at frequency  $\nu$ ,  $k_{\text{B}}$  is Boltzmann's constant and  $\Omega$  the solid angle subtended by the source. Our most stringent constraint

<sup>1</sup> [http://vlbi.gsfc.nasa.gov/solutions/2005f\\_astro/2005f\\_astro\\_cat.txt](http://vlbi.gsfc.nasa.gov/solutions/2005f_astro/2005f_astro_cat.txt)



comes from the microflare, when the flux density measured by the HSA was  $1.0 \pm 0.1$  mJy and fitting an elliptical Gaussian to the source in the image plane gave an upper limit to the source size of  $1.8 \times 1.7$  mas<sup>2</sup>. This gives a lower limit to the brightness temperature of  $T_b > 1.1 \times 10^7$  K. For comparison, for the non-flaring data, fitting an elliptical Gaussian in the image plane gave an upper limit to the size of  $2 \times 0.6$  mas<sup>2</sup> and a consequent lower limit to the brightness temperature of  $7 \times 10^6$  K.

Previous VLBI observations of Galactic X-ray binary jets have measured brightness temperatures of  $\geq 10^9$  K (e.g. Dhawan et al. 2000; Mirabel et al. 2001). Should this be the case in V404 Cyg, we can use the flux density during the flare to place an upper limit of  $4.6 \times 10^{-19}$  sr on the solid angle subtended by the source, corresponding to a geometric mean size of 0.16 mas. However, most resolved X-ray binary systems have shown collimated jets, so as an example, for an axial ratio of 4:1 (the definition of jets adopted by Bridle & Perley 1984), the derived solid angle would translate into a jet length of 0.3 mas.

The inverse Compton catastrophe limits the brightness temperature of a radio-emitting source to  $< 10^{12}$  K, if it is not relativistically boosted. For the flux density of  $1.0$  mJy beam<sup>-1</sup> measured during the flare, this limits the source size to  $> 5 \mu\text{as}$  ( $> 2 \mu\text{as}$  for the non-flaring emission with a flux density of  $0.24$  mJy beam<sup>-1</sup>).

### 4.3 Variability limits

The  $< 30$ -min rise time of the flare corresponds to a distance of  $5.4 \times 10^{11}$  m for a source moving at the speed of light, or an angular size of 0.9 mas if the motion is in the plane of the sky. However, sources moving at small angles to the line of sight can show apparent superluminal motion, with  $\beta_{\text{app}} > 1$ . We have no constraints on the speed or inclination angle to the line of sight of the source, but constrain the size of the flaring region to be  $< 0.9\beta_{\text{app}}$  mas.

Similarly, for the brightness temperature size constraints derived in Section 4.2, we can derive limits on the jet speed, for a rise time of 30 min. For  $T_B \geq 10^9$  K, the jet speed is limited to  $< 0.33c$ , and for  $T_B < 10^{12}$  K, the jet speed is  $> 830$  km s<sup>-1</sup>. If the jet is to be moving close to the speed of light, it would have to be more elongated, and have a lower brightness temperature.

### 4.4 Theoretical limits

Heinz (2006) derived an expression for the length of a flat-spectrum, partially self-absorbed jet, as a function of basic jet parameters, normalizing the relation using the VLBA measurements of the jet in Cygnus X-1 (Stirling et al. 2001). The observed angular extent of the jet,  $\mu_{50\%}$ , within which 50 per cent of the flux density is contained, can be written as

$$\mu_{50\%} \propto \left( \frac{S_\nu^8 (\sin \theta)^{10}}{d \delta^2} \right)^{1/17} \text{ mas}, \quad (2)$$

where  $d$  is the source distance,  $\delta = [\Gamma(1 - \beta \cos \theta)]^{-1}$  is the Doppler factor,  $\theta$  the inclination angle of the jet to the line of sight,  $\Gamma$  the Lorentz factor  $(1 - \beta^2)^{-1/2}$ , and  $\beta = v/c$  is the jet velocity in units of the speed of light. Shahbaz et al.

(1994) derived an inclination angle of  $56 \pm 4^\circ$  for V404 Cyg, and we measured a flux density of 0.3 mJy. Heinz (2006) took values of  $\mu_{50\%} = 3$  mas,  $S_\nu = 12$  mJy and  $\theta = 35^\circ$  for Cygnus X-1. With these parameters, a distance of 4 kpc, and assuming that the Doppler factor is similar in the two sources (since  $\mu_{50\%}$  scales as  $\delta^{-2/17}$ , the exact value is unimportant) and that the disc is perpendicular to the jet, we predict a jet length of 0.6 mas in V404 Cyg.

### 4.5 Previous constraints

Mioduszewski et al. (2008) also observed V404 Cyg with the VLBA and phased VLA. From their non-detection at 15 GHz, when the VLA lightcurve suggested that an  $8\sigma$  source should have been seen, they inferred that the source was being resolved out, putting a lower limit on the source size of 1 mas. Together with light-travel time arguments applied to the flares they detected, they constrained the source size to lie in the range 4–7 AU. While this is consistent with our upper limit of 1.3 mas, it might initially appear to be difficult to reconcile with the theoretical predictions of 0.3–0.6 mas. Either the models are out by a factor of 2–3 (quite possible given some of the inherent assumptions), or some unknown instrumental problem (possibly similar to the apparent suppression of the flux density we found when using the VLA during the flare) caused the source brightness to be reduced below their expected  $8\sigma$  detection. In order to resolve the jet, high-frequency, global VLBI would be required, to overcome the scattering (which scales as  $\nu^{-2}$ ) and achieve a resolution of  $\leq 1$  mas. Should the jets not be detected with higher-resolution observations, it would present a serious challenge to the jet interpretation of the radio emission from quiescent systems.

## 5 SCATTERING

The line of sight to the Cygnus region is known to be highly scatter-broadened (Fey et al. 1989). Fluctuations in the electron density in the interstellar medium (ISM) modify the refractive index of the plasma, inducing distortions in a wavefront travelling through the medium. This reduces the coherence of the electric field measured by two separated antennas, reducing the amplitude of the visibilities measured on long baselines, or, equivalently, giving rise to angular broadening in the image plane. Rickett (1990) discusses other effects of interstellar scattering, such as scintillation and temporal broadening of pulsed emission.

Fey et al. (1989) measured the scattering properties along the lines of sight to several extragalactic calibrators in the Cygnus region, including our phase reference source, J 2025+3343 (i.e. B 2023+336) and our amplitude check source, J 2023+3153 (i.e. B 2021+317). The scattering is clearly non-uniform, and the scattering properties can differ dramatically with small position offsets on the sky. Between our two calibrators, separated by only  $1.9^\circ$ , the scattering measure varies by a factor of five. The measured scattering size of J 2025+3343 at 4.99 GHz was  $2.9 \pm 0.7$  mas, scaling as  $\nu^\gamma$ , with  $\gamma = -1.97 \pm 0.29$ . At 8.4 GHz, we measured a scattering disc size of  $2.2 \times 1.4$  mas<sup>2</sup>, fitting in either the image or  $uv$ -plane. This is significantly larger than the previously-derived scattering size, although the size is

known to vary; Fey & Desai (2000) claimed evidence for a 50 per cent increase in scattering disc size at all frequencies, in observations taken three years after their original data.

### 5.1 Source distance

V404 Cyg lies behind the Cygnus superbubble. Uyaniker et al. (2001) found that the superbubble was not a single physical entity, but a projection of unrelated features at different distances. Nevertheless, the structures are all believed to lie between 0.5 and 2.5 kpc from us. While the line of sight to V404 Cyg does not pass through any of the known OB associations in the region, we can limit the location of the major scattering screen to be within the same range of distances. Assuming a single thin phase screen is responsible for the majority of the scattering, then according to the relative distance of the scattering screen and scattered source, we can predict the expected scattering size,

$$\theta_{\text{gal}} = \left(1 - \frac{d_s}{d}\right)\theta_{\text{xgal}}, \quad (3)$$

where  $\theta_{\text{gal}}$  is the scattering size of the galactic source at distance  $d$ ,  $\theta_{\text{xgal}}$  is the scattering size of the background extragalactic source, and  $d_s$  is the distance from the observer to the phase screen. As demonstrated by Lazio & Cordes (1998), the observed scattering size of a galactic source depends on the relative distance of the source and the intervening phase scattering screen. The closer the source is to the scattering screen, the less scattered the source will be.

The major axis of the calibrator scattering disc, 2.2 mas, together with the maximum major axis size of  $\sim 1.3$  mas permitted by the fits to the source data in the image and  $uv$  planes shows that if the assumption of a thin phase screen is valid, and the scattering measure is similar along the lines of sight to the source and calibrator, then the lower limit to the source distance is  $d < 2.4d_s$ . This gives limits of  $< 1.2$  and  $< 6.1$  kpc respectively, for screen distances of 0.5 and 2.5 kpc, consistent with the range of 2.8–6.2 kpc range derived by Jonker & Nelemans (2004). While this is not terribly constraining, it shows that lower-frequency observations which resolved the scattering disc of V404 Cyg could potentially provide an alternative, albeit model-dependent, estimate of the source distance.

### 5.2 Scintillation

Given the high scattering towards the source, we should determine whether the observed variability is intrinsic to the source, or whether it could be caused by interstellar scintillation. From the scattering measure of  $SM_0 = 0.34 \pm 0.12 \text{ m}^{-20/3} \text{ kpc}$  measured towards the phase reference source by Fey et al. (1989), and assuming a scattering screen located at  $d_0 = 0.5$  kpc, then the standard scattering equations (e.g. Goodman 1997) imply that we are in the strong scattering regime (for which the cutoff frequency is  $\nu < 100(d_s/d_0)^{5/17}(SM/SM_0)^{6/17} \text{ GHz}$  with these parameters). Our observing bandwidth of 32 MHz is too large to detect diffractive scintillation (the decorrelation bandwidth is  $1.6(d_s/d_0)^{-1}(SM/SM_0)^{-6/5} \text{ MHz}$ ), and the source size, limited to  $> 5 \mu\text{as}$  by the inverse Compton limit of  $T_b = 10^{12} \text{ K}$ , is also too large (diffractive scattering would

require  $\theta < 0.06(d_s/d_0)^{-1}(SM/SM_0)^{-3/5} \mu\text{as}$ ). Thus we are in the regime of refractive scintillation. For intrinsic source sizes between  $5 \mu\text{as}$  and  $1.3 \text{ mas}$  (from the brightness temperature limit and the measured upper limit on the source size from the visibilities), the timescale of refractive scintillation is between 140 and 1000 h (scaling almost linearly with  $d_s$ ), with a modulation index  $0.02 < m_R < 0.18$  (scaling as  $\sim (d_s/d_0)^{-1/6}(SM/SM_0)^{1/2}$ ). Thus the observed variability, an increase by a factor of 3 on a timescale  $< 1$  h, must be intrinsic to the source.

## 6 FLARING AND THE NATURE OF THE QUIESCENT STATE

Despite being in a “quiescent” state, V404 Cyg exhibits sub-orbital variability in the optical (Wagner et al. 1992) and infrared (Sanwal et al. 1996) bands, with some evidence for a 6-h quasi-periodicity (Casares et al. 1993). Hynes et al. (2002) found that variable photo-ionization of the accretion disc by the X-ray source was responsible for the observed H $\alpha$  flares, a conclusion reinforced by observations of correlated X-ray and H $\alpha$  variability (Hynes et al. 2004). The optical continuum flares did not correlate as well with the X-ray flares, leading Hynes (2005) to suggest that the continuum variability could be due to synchrotron emission from a jet. The source is known to vary in the radio band (e.g. Hjellming et al. 2000), and Mioduszewski et al. (2008) presented tentative evidence for a similar 6-h radio periodicity. The similar variability characteristics (timescales and flare amplitudes) seen at the different wavebands are suggestive of a common origin.

While certainly intrinsic to the source, and clearly a common phenomenon in this system, the nature of the radio flaring is still to be determined. A thermal bremsstrahlung origin is ruled out, since it would produce too high an X-ray luminosity for the system. This suggests that the radio emission is non-thermal (certainly plausible given the relatively high brightness temperature), although a spectral index measurement during a flare is needed to determine whether such flares are optically thick or optically thin. Due to a paucity of simultaneous multiwavelength observations, any connection with the optical continuum flares remains purely speculative. We note, however, evidence for a correlation between the optical and radio bands is seen in the identical power-law decay timescale measured in the two wavebands during the 1989 outburst (Han & Hjellming 1992).

The  $< 30$  min rise time of the flare implies that the source of the flaring emission must be of size  $< 4 \text{ AU}$ ,  $\sim 20$  times the size of the binary orbit (Shahbaz et al. 1994). Mioduszewski et al. (2008) suggested three possibilities for the origin of such flaring; collimated jets, shocks in the circumstellar medium, or diffuse emission as seen in SS 433 (Blundell et al. 2001). The latter was on much larger scales (several hundred AU), and was interpreted by the authors as bremsstrahlung emission, for which reasons, we are inclined to favour the jet or shock interpretations.

The flat radio spectrum seen in the quiescent state of V404 Cyg (Gallo et al. 2005) implies optically-thin thermal or optically-thick synchrotron emission. Thermal emission is ruled out due to overpredicting the observed X-ray emission. Optically-thick synchrotron emission is typically interpreted

as a partially self-absorbed conical jet in X-ray binary systems, which would make flaring in the jet, possibly due to internal shocks, a potential candidate for the observed variability. Other circumstantial evidence for the existence of jets in the quiescent state is seen in the correlation between the X-ray and radio luminosities of hard-state black hole X-ray binaries at X-ray luminosities below  $L_x \sim 0.01L_{\text{Edd}}$  (Gallo et al. 2003). This correlation was later demonstrated to hold across the entire black hole mass spectrum (Merloni, Heinz & di Matteo 2003; Falcke, Körding & Markoff 2004), and simultaneous X-ray and radio observations of A0620-00 (Gallo et al. 2006) demonstrated that this correlation persists in quiescence, down to X-ray luminosities as low as  $10^{-8.5}L_{\text{Edd}}$ . The resolved jets seen in GRS1915+105 and Cygnus X-1 at the high-luminosity end of the correlation then make it plausible that jets are also present at much lower luminosities. However, there are several caveats to this argument. A number of sources have recently been found with lower than expected radio luminosities (Corbel et al. 2004; Chaty 2006; Cadolle Bel et al. 2007; Rodriguez et al. 2007), calling into question the universality of the correlation (Gallo 2007). Also, in the absence of direct imaging, nothing is known about the extent and degree of collimation of such quiescent jets, should they exist. The inferred larger inner disc radii derived in the quiescent state (McClintock et al. 2003) could potentially affect the collimation of the outflow. While the SED of the quiescent source A0620-00 has been well-fitted with a maximally jet-dominated model (Gallo et al. 2007), other models cannot be ruled out. Extended, flat-spectrum radio emission not arising from a jet has been seen in the relatively uncollimated expanding structures observed in CI Cam (Mioduszewski & Rupen 2004) and RS Oph (Rupen et al. 2007) and the equatorial emission of SS 433 (Blundell et al. 2001). Thus the true morphology of the emission in V404 Cyg cannot be definitively ascertained without high-resolution radio imaging.

Han & Hjellming (1992) suggested that the short-timescale variability in the radio lightcurves of the 1989 outburst of V404 Cyg could be interpreted as shocks at the ends of jets. Circumstellar shocks have been directly imaged in the high-mass X-ray binary CI Cam (Mioduszewski & Rupen 2004). This system has a very dense stellar wind, which is thought to have smothered the jets ejected during the outburst, giving rise to an expanding shell of radio emission seen on VLBI scales. While the wind in V404 Cyg is likely to be less strong, the size constraint on the flares of V404 Cyg implies that they are occurring closer to the binary than the shock seen in CI Cam, where any wind from the donor star would be densest. With the available single-frequency, unresolved radio image, we cannot hope to pin down the location of the shocks. Ultimately, some explosive event is required to cause the radio flares, and whether they are shocks within or at the ends of jets cannot yet be determined.

As the most luminous black hole X-ray binary in quiescence, V404 Cyg is the only source in which such flaring activity has been detected in the quiescent state. The question of whether the flares are unique to this source, or are commonplace in such systems, has implications for the nature of the accretion process at low luminosities. Owing to the limitations of current instrumentation, it has not been possible to observe other quiescent systems with sufficient time reso-

lution in the radio band to detect such flares. Models fitting the SEDs of quiescent sources often assume a non-varying source, such that non-simultaneous observations in different bands could be used to build up the SED (e.g. Gallo et al. 2007). If flaring emission is ubiquitous in these sources, the need for strict simultaneity will have to be more rigorously enforced.

Observations of XTE J1118+480 and GX 339-4 in their hard states (currently differentiated from the quiescent state only by a fairly arbitrary luminosity criterion) have shown evidence for fast variability in the optical and X-ray regimes (Motch et al. 1983; Hynes et al. 2003). In XTE J1118+480, both the autocorrelations and the cross-correlation between the two wavebands were inconsistent with X-ray reprocessing and more indicative of optical synchrotron variability (Kanbach et al. 2001), which Malzac, Merloni & Fabian (2004) were able to explain with a jet-dominated model. The timescales are shorter in this source than seen in V404 Cyg however, and there were no high-time resolution radio data for comparison (although we note that we would not expect to see radio variability on timescales shorter than a few minutes, since any variations occurring at the base of a jet would be smoothed out further downstream where the source became optically thin in the radio regime). A better comparison is the quiescent black hole in the centre of our Galaxy, Sgr A\*, accreting at  $\sim 10^{-8}L_{\text{Edd}}$ . It shows radio and infrared flaring activity (although any connection between the two bands is as yet unclear), and the radio flaring has been explained as adiabatic expansion of a self-absorbed transient population of relativistic electrons (e.g. Yusef-Zadeh et al. 2006).

There is thus significant evidence that flaring activity in or at the end of a jet is a feature of the quiescent state of accreting black hole systems. Whether there is a truly steady underlying jet as assumed by standard jet models (Blandford & Königl 1979) or whether the emission is composed of multiple overlapping flares, or some more uncollimated structure, remains to be determined. More sensitive instruments such as the Expanded VLA (EVLA), e-MERLIN and the upgraded VLBA are necessary to probe these short-timescale flares and determine the nature of the quiescent emission.

## 7 CONCLUSIONS

We have detected the quiescent black hole X-ray binary system V404 Cyg with the High Sensitivity Array at 8.4 GHz. The unresolved source has a brightness temperature of  $> 10^7$  K, and the emission is inferred to be non-thermal synchrotron radiation. Our detection provides the most accurate source position to date, which can serve as an initial point for future proper motion studies. We have also constrained the length of the jet in this system to be  $< 1.3$  mas, consistent with previous measurements and theoretical expectations.

A small flare was detected with both the VLA and the HSA, with a rise timescale of 30 min, in which the source flux density rose by a factor of 3. This flare is certainly intrinsic to the source, and cannot be caused by interstellar scintillation. This is further evidence that source flux densities in the quiescent state are not stable, mandating the

use of strictly simultaneous observations when constructing and modelling SEDs to determine the contribution of different components (such as jets) to the observed emission in different wavebands.

The detection of an unresolved quiescent black hole X-ray binary system opens the way for further high-resolution observations. If the inferred jets indeed exist, and are flat-spectrum, as has been proposed, then higher-frequency observations would be well-placed to resolve the jets, if the theoretical predictions for the jet length are correct. Furthermore, the unresolved source at 8.4 GHz is an ideal candidate for a parallax distance determination, free from the uncertainties associated with the source structure seen when such systems are observed with VLBI during outburst.

## ACKNOWLEDGMENTS

This research has made use of NASA's Astrophysics Data System. J.C.A.M.-J. is a Jansky Fellow of the National Radio Astronomy Observatory. E.G. is supported through Chandra Postdoctoral Fellowship grant number PF5-60037, issued by the Chandra X-Ray Center, which is operated by the Smithsonian Astrophysical Observatory for NASA under contract NAS8-03060. The VLBA is a facility of the National Radio Astronomy Observatory which is operated by Associated Universities, Inc., under cooperative agreement with the National Science Foundation.

## REFERENCES

- Benz A. O., Güdel M., 1994, *A&A*, 285, 621  
 Blandford R. D., Konigl A., 1979, *ApJ*, 232, 34  
 Blundell K. M., Mioduszewski A. J., Muxlow T. W. B., Podsiadlowski P., Rupen M. P., 2001, *ApJ*, 562, L79  
 Bridle A. H., Perley R. A., 1984, *ARA&A*, 22, 319  
 Bradley C. K., Hynes R. I., Kong A. K. H., Haswell C. A., Casares J., Gallo E., 2007, *ApJ*, 667, 427  
 Cadolle Bel M. et al., 2007, *ApJ*, 659, 549  
 Casares J., Charles P. A., 1994, *MNRAS*, 271, L5  
 Casares J., Charles P. A., Naylor T., Pavlenko E. P., 1993, *MNRAS*, 265, 834  
 Chaty S., 2006, in Belloni T., ed., *Proceedings of the "VI Microquasar Workshop: Microquasars and Beyond"*, PoS: Trieste, 14  
 Corbel S., Fender R. P., Tomsick J. A., Tzioumis A. K., Tingay S., 2004, *ApJ*, 617, 1272  
 Corbel S., Tomsick J. A., Kaaret P., 2006, *ApJ*, 636, 971  
 Desai K. M., Fey A. L., 2001, *ApJS*, 133, 395  
 Dhawan V., Mirabel I. F., Rodríguez, L. F. 2000, *ApJ*, 543, 373  
 Falcke H., Körding, E., Markoff S., 2004, *A&A*, 414, 895  
 Fender R. P., 2001, *MNRAS*, 322, 31  
 Fey A. L., Desai K. M., 2000, *BAAS*, 197, 722  
 Fey A. L., Spangler S. R., Mutel R. L., 1989, *ApJ*, 337, 730  
 Gallo E., Fender R. P., Pooley G. G., 2003, *MNRAS*, 344, 60  
 Gallo E., Fender R. P., Hynes R. I., 2005, *MNRAS*, 356, 1017  
 Gallo E., Fender R. P., Miller-Jones J. C. A., Merloni A., Jonker P. G., Heinz S., Maccarone T. J., van der Klis M., 2006, *MNRAS*, 370, 1351  
 Gallo E., 2007, in L.A. Antonelli et al., *AIP Conf. Ser.* 924, *The multicolored landscape of compact objects and their explosive origins*, AIP, New York, p.715  
 Gallo E., Migliari S., Markoff S., Tomsick J. A., Bailyn C. D., Berta S., Fender R., Miller-Jones J. C. A., 2007, *ApJ*, 670, 600  
 Garcia M. R., McClintock J. E., Narayan R., Callanan P., Barret D., Murray S. S., 2001, *ApJ*, 553, L47  
 García-Sánchez, J., Paredes J. M., Ribó M., 2003, *A&A*, 403, 613  
 Goodman J., 1997, *New Astronomy*, 2, 449  
 Greisen E. W., 2003, in *Information Handling in Astronomy: Historical Vistas*, ed. A. Heck (Dordrecht: Kluwer), 109  
 Güdel, M., 2002, *ARA&A*, 40, 217  
 Han X., Hjellming R. M., 1992, *ApJ*, 400, 304  
 Heinz S., 2006, *ApJ*, 636, 316  
 Hjellming R. M., Johnston K. J., 1988, *ApJ*, 328, 600  
 Hjellming R. M., Rupen M. P., Mioduszewski A. J., Narayan R., 2000, *ATel.* 54  
 Hynes R. I., 2005, in *ASP Conf. Ser.* 330, *The Astrophysics of Cataclysmic Variables and Related Objects*, eds. J. M. Hameury & J.-P. Lasota, (San Francisco: Astronomical Society of the Pacific), 237  
 Hynes R. I., Zurita C., Haswell C. A., Casares J., Charles P. A., Pavlenko E. P., Shugarov S. Y., Lott D. A., 2002, *MNRAS*, 330, 1009  
 Hynes R. I. et al., 2003, *MNRAS*, 345, 292  
 Hynes R. I. et al., 2004, *ApJ*, 611, L125  
 Jonker P. G., Nelemans G., 2004, *MNRAS*, 354, 355  
 Kanbach G., Straubmeier C., Spruit H. C., Belloni T., 2001, *Nature*, 414, 180  
 Kong A. K. H., McClintock J. E., Garcia M. R., Murray S. S., Barret D., 2002, *ApJ*, 570, 277  
 Lazio T. J. W., Cordes J. M., 1998, *ApJS*, 118, 201  
 Malzac J., Merloni A., Fabian A. C., 2004, *MNRAS*, 351, 253  
 McClintock J. E., Remillard R. A., 2006, in *Compact stellar X-ray sources*, ed. W. H. G. Lewin & M. van der Klis (Cambridge: Cambridge University Press), 157  
 McClintock J. E., Narayan R., Garcia M. R., Orosz J. A., Remillard R. A., Murray S. S., 2003, *ApJ*, 593, 435  
 Merloni A., Heinz S., di Matteo T., 2003, *MNRAS*, 345, 1057  
 Mioduszewski A. J., Rupen M. P., 2004, *ApJ*, 615, 432  
 Mioduszewski A. J., Hynes R. I., Rupen M. P., Dhawan V., 2008, in *AIP Conf. Ser.*, *A Population Explosion: The Nature and Evolution of X-ray Binaries in Diverse Environments*, eds. R. M. Bandyopadhyay, S. Wachter & D. M. Gelino & C. R. Gelino (New York: American Institute of Physics),  
 Mirabel I. F., Dhawan V., Mignani R. P., Rodrigues I., Guglielmetti F., 2001, *Nature*, 413, 139  
 Motch C., Ricketts M. J., Page C. G., Ilovaisky S. A., Chevalier C., 1983, *A&A*, 119, 171  
 Muno M. P., Mauerhan J., 2006, *ApJ*, 648, L135  
 Mutel R. L., Morris D. H., Doiron D. J., Lestrade J. F., 1987, *AJ*, 93, 1220  
 Richards M. T., Waltman E. B., Ghigo F. D., Richards D. S. P., 2003, *ApJS*, 147, 337



- Rickett B. J., 1990, *ARA&A*, 28, 561
- Rodriguez J., Bel M. C., Tomsick J. A., Corbel S., Brock-sopp C., Paizis A., Shaw S. E., Bodaghee A., 2007, *ApJ*, 655, L97
- Rupen M. P., Mioduszewski A. J., Sokoloski J. L., *ApJ*, accepted
- Sanwal D., Robinson E. L., Zhang E., Colome C., Harvey P. M., Ramseyer T. F., Hellier C., Wood J. H., 1996, *ApJ*, 460, 437
- Shahbaz T., Ringwald F. A., Bunn J. C., Naylor T., Charles P. A., Casares J., 1994, *MNRAS*, 271, L10
- Shahbaz T., Bandyopadhyay R., Charles P. A., Naylor T., 1996, *MNRAS*, 282, 977
- Stirling A. M., Spencer R. E., de la Force C. J., Garrett M. A., Fender R. P., Ogle R. N., 2001, *MNRAS*, 327, 1273
- Strassmeier K. G., Hall D. S., Fekel F. C., Scheck M., 1993, *A&AS*, 100, 173
- Uyaniker, B., Fürst, E., Reich W., Aschenbach B., Wielebinski R., 2001, *A&A*, 371, 675
- Wagner R. M., Kreidl T. J., Howell S. B., Starrfield S. G., 1992, *ApJ*, 401, L79
- Yusef-Zadeh F., Roberts D., Wardle M., Heinke C. O., Bower G. C., 2006, *ApJ*, 650, 189